

Electrochemical Investigations of M-DNA Self-Assembled Monolayers on Gold Electrodes

Chen-Zhong Li,^{†‡} Yi-Tao Long,^{†‡} Heinz-Bernhard Kraatz,^{*,†} and Jeremy S. Lee^{*,‡}

Department of Chemistry, University of Saskatchewan, 110 Science Place, Saskatoon, SK, Canada S7N 5C9, and Department of Biochemistry, University of Saskatchewan, 107 Wiggins Road, Saskatoon, SK, Canada S7N 5E5

Received: August 19, 2002; In Final Form: December 5, 2002

Monolayers of double-stranded DNA on polycrystalline gold electrodes were prepared by chemisorbing SS-5'-GTCACGATGGCCAGTAGTT-3' (1) hybridized with its complementary strand 5'-AACTACTGGGC-CATCGTGAC-3' (2) onto gold through a disulfide linkage, giving a monolayer with hydroxylalkyl chains adjacent to the double-stranded DNA (ds-DNA). The system forms a stable and well-behaved ds-DNA monolayer on gold, which reduces the signal transduction between a solution electrophore and the gold surface. Upon addition of Zn²⁺ to the solution at pH 8.6, Zn²⁺ associates with the ds-DNA and form M-DNA. In contrast to ds-DNA, the signal transduction is significantly enhanced. The heterogeneous electron-transfer rate (k_{ET}) between the ferricyanide electrophore and the surface was determined for bare gold, ds-DNA, and M-DNA monolayers. k_{ET} for electron transfer from the solution electrophore to the gold surface through the M-DNA monolayer is $1.2 \times 10^{-4} \pm 0.2 \times 10^{-4} \text{ cm s}^{-1}$, which is smaller than for bare gold under the same conditions ($k_{ET} = 9.1 \times 10^{-4} \pm 0.2 \times 10^{-4} \text{ cm s}^{-1}$). For simple ds-DNA, k_{ET} was too slow to be measured.

Introduction

The electron-transfer properties of various biomolecules such as proteins, peptides, and DNA have attracted a significant amount of attention over the past few years, largely driven by the desire to develop devices able to detect mutations or to prepare nanoscale biological devices such as molecular wires.^{1–4} In particular, the conductivity of double-stranded DNA (ds-DNA) has been studied in detail. The results were often contradictory—some reports have indicated that ds-DNA is a conductor and mediates electron transfer via the π -stacked base pairs whereas other reports suggested that DNA is an insulator under certain conditions.^{5,6}

Recent reports of the direct measurements of electrical transport through a 10.4-nm ds-DNA oligomer⁷ demonstrate that ds-DNA is a semiconductor with a wide band gap. Although native DNA is an inadequate conductor, it can be improved by coating individual DNA fibers with metallic silver.⁸ A novel method for improving the conductivity of DNA was reported recently and involves close association or even incorporating divalent metal ions such as Zn²⁺, Ni²⁺, and Co²⁺ into the helix at pH > 8.5 to form metalated DNA (M-DNA).^{9,10} Other divalent metals such as Mg²⁺ and Ca²⁺ do not form M-DNA. In photophysical studies using ds-DNA where one strand is labeled with a fluorescein fluorophore and the complementary strand carries a rhodamine quencher, the fluorescein fluorescence is quenched only under conditions where M-DNA forms. Preliminary evidence demonstrates that M-DNA is an efficient conductor of electrons over distances as long as 500 base pairs and possibly as long as several micrometers.⁹ It is proposed that in M-DNA the Zn²⁺ cations replace the imino protons of every thymine and guanine in addition to saturating the

backbone phosphates as do other cations such as Mg²⁺.¹⁰ M-DNA can be converted back to ordinary ds-DNA by the addition of ethylenediaminetetraacetic acid (EDTA) to remove the metal ions.

Electrochemical techniques have proven invaluable for probing the electron-transfer properties of immobilized biomolecules and have yielded information regarding the electron-transfer kinetics and potential pathways.^{11,12} The immobilization of DNA on an electronically conductive substrate has been described in the literature.^{13–16} In particular, DNA linked to a gold surface through a Au–S linkage will often form very stable monolayer assemblies with a well-defined 2D structure.^{17–21}

Stable monolayers on gold have been formed from alkylthiols and disulfides, giving what is believed to be a stable alkylthiolate–gold linkage.^{22,23} However, the possibility of a disulfide bond coordinating to the surface cannot be excluded.^{24a}

Here we provide a detailed account of our study of the electrochemical properties of M-DNA supported on gold surfaces, including the examination of the electron-transfer kinetics. Our kinetic studies demonstrate that M-DNA allows electron transfer more facile than ds-DNA.

Experimental Section

General. [Ru(NH₃)₆]Cl₃, [Ru(NH₃)₆]Cl₄, K₃[Fe(CN)₆], and K₄[Fe(CN)₆] were purchased from Aldrich and used without further purification. Zn(ClO₄)₂, Mg(ClO₄)₂, and tris-ClO₄ were purchased from Fluka Co. Deionized water (18 M Ω cm resistivity) from a Millipore Milli-Q system was used throughout this work.

Oligonucleotide Synthesis. HO–(CH₂)₆SS(CH₂)₆OPO₃H was used to modify the oligonucleotides at the 5' terminus. The 5'-modified oligonucleotides and underivatized complements used in the study were synthesized by standard phosphoramidite chemistry²⁵ using a fully automated DNA synthesizer at the Plant Biotechnology Institute (PBI-NRC, Saskatoon). The oligonucleotides were purified by two-step reversed-phase

* Corresponding authors. E-mail: kraatz@skyway.usask.ca. Fax: +306-966-4730.

[†] Department of Chemistry, University of Saskatchewan.

[‡] Department of Biochemistry, University of Saskatchewan.

HPLC and then characterized by MALDI-TOF. The sequences and nomenclature used are as follows:

SS-5'-GTCACGATGGCCAGTAGTT-3' 1

5'-AACTACTGGGCCATCGTGAC-3' 2

Note: SS 5' refers to $\text{HO}_3\text{PO}-(\text{CH}_2)_6\text{-SS}-(\text{CH}_2)_6\text{-OH}$

Electrode Characterization and Pretreatment. Gold disk electrodes (Bioanalytical Systems Inc., 1.6-mm diameter, ca. 0.02 cm^2 geometrical area, and roughness coefficients of 1.2–1.4) were used for the electrochemical measurement. Before modification, the electrode surface was cleaned by electrochemical sweeping in 0.1 M H_2SO_4 from 0 to 1.4 V, rinsed with water, and then ultrasonicated for 5 min in fresh piranha solution (30% H_2O_2 , 70% H_2SO_4). *Warning: Piranha solution reacts violently with organic solvents.* The electrode was then sonicated by freshly distilled and degassed ethanol and then rinsed with Milli-Q water. A cyclic voltammogram recorded in 0.1 M H_2SO_4 (scan rate 100 mV s^{-1}) was used to determine the active area of the electrode surface. The real electrode surface area and roughness factors were obtained by integrating the gold oxide reduction peak.^{26,27} The gold oxide was reduced in situ to a clean gold surface by immersion in degassed freshly distilled ethanol.

Preparation of DNA SAMs. ds-DNA was hybridized in 20 mM tris- ClO_4 (pH 8.6) from disulfide-modified DNA 1 and its complementary strand 2 at room temperature for 10 h. Hybridization was confirmed by the ethidium fluorescence assay.²⁸ The cleaned gold electrodes (vide supra) were immersed in an aqueous solution of tris- ClO_4 (100 mM), NaClO_4 (100 mM), and the hybridized ds-DNA conjugate at pH 8.6. The concentration of the DNA was 0.2 mM. After 3 days, the electrodes were repeatedly rinsed with tris- ClO_4 (50 mM, pH 8.6) for 5 min. The resulting electrode was then soaked again in the same ds-DNA solution overnight and rinsed with buffer three times. The derivatized electrode surface coverage was quantified to be over 90% by the underpotential deposition (UPD) of Cu.^{29–31} The ds-DNA monolayer was converted into the M-DNA monolayer by exposing the monolayer to a solution of 0.3 mM $\text{Zn}(\text{ClO}_4)_2$ in 20 mM tris- ClO_4 buffer (pH 8.6) for at least 2 h.

Electrochemical Measurements. All electrochemical experiments were performed in a conventional three-electrode cell consisting of the DNA-SAM-modified Au electrode as the working electrode, a Ag/AgCl/3 M NaCl reference electrode (BAS), and a platinum wire auxiliary electrode. All potentials are reported with the respect to the Ag/AgCl/3 M NaCl reference electrode. A BAS 50-W potentiostat was used for the electrochemical measurements. Typical CV experiments employed a 5 mM solution of $[\text{Ru}(\text{NH}_3)_6]\text{Cl}_4/[\text{Ru}(\text{NH}_3)_6]\text{Cl}_3$ or a 2.5 mM solution of $\text{K}_3[\text{Fe}(\text{CN})_6]/\text{K}_4[\text{Fe}(\text{CN})_6]$ in 20 mM tris- ClO_4 solution at pH 8.6 with or without divalent M^{2+} at room temperature ($20 \pm 2^\circ\text{C}$). The open-circuit or rest potential of the system was measured prior to all electrochemical experiments to prevent sudden potential-related changes in the SAM. All electrochemical experiments were started from the rest potential. UPD experiments were carried out in 1 mM $\text{Cu}(\text{ClO}_4)_2$ in 0.1 M HClO_4 at a scan rate of 10 mV s^{-1} starting at 500 mV (vs Ag/AgCl) followed by cathodic scanning to 50 mV and an anodic sweep to 600 mV. Simulation of the CV curves was done using the DigiSim 21 simulation program (BAS).

Results and Discussion

The oligonucleotide SS-5'-GTCACGATGGCCAGTAGTT-3' (1) and its complementary strand 5'-AACTACTGGGC-

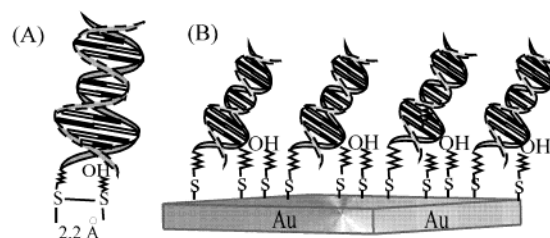


Figure 1. Schematic representation of (A) the model of di-6-alkyl disulfide-modified double-stranded DNA giving rise to (B) the proposed model of the mixed SAMs on a gold surface.

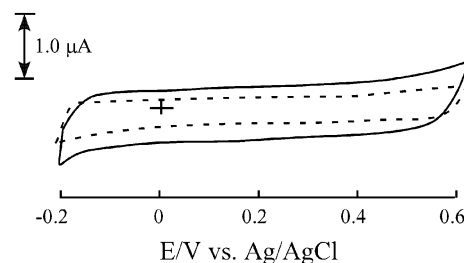


Figure 2. Comparison of the capacitive background currents on bare (—) and ds-DNA-modified gold electrode (---) in 20 mM tris- ClO_4 buffer solution (pH 8.6) at a sweep rate of 100 mV s^{-1} .

CATCGTGAC-3' (2) were synthesized by automated solid-phase synthesis. Chemisorption of the ss-DNA-hydroxyalkyl disulfide 1 or the ds-DNA prepared by the hybridization of 1 and 2 resulted in a mixed monolayer having DNA-thiolate and hydroxyalkylthiolate-gold linkages with the DNA thiolate adjacent to the hydroalkylthiolate residue, as indicated in Figure 1. Experimental evidence by others strongly suggests that S–S bond cleavage occurs upon chemisorption.^{24b,c} Nonspecifically bound DNA was readily removed by washing with buffer.¹⁹

It is predicted that this arrangement should prevent the interaction of DNA with the gold surface through the nitrogen of the nucleotides.³² Furthermore, the disulfide adsorption should result in a more uniform monolayer structure.²⁴ Usually “dilute” DNA monolayers are prepared by soaking a monolayer prepared from DNA-thiol in a solution of alkylthiol solution.^{18,33,34} This result is a two-component film, which often shows phase separation and incomplete mixing of the two components on the surface. Furthermore, this procedure leads to a displacement of the bound DNA-thiolate by the alkylthiol.^{19,34} In the present study, unlike previous studies, systems derived from the asymmetric DNA conjugate 1 were used to modify the electrode surface. In particular, the choice of the terminal hydroxyl function of the alkyl appears to play an important role in determining the monolayer stability and packing.^{35,36} The terminal OH groups appear to be an essential element in the production of stable monolayers. H-bonding interactions involving HO-PO_3 in monolayer systems containing cystamine were reported before and lead to very stable monolayer systems.^{37,38}

At the DNA-modified electrodes, the capacitive background currents (Figure 2) are smaller compared to those of a bare gold electrode, as expected for the presence of a monolayer with a low dielectric constant.

Figure 3 shows the results of a UPD study of Cu on bare gold and a ds-DNA-modified gold electrode taken in 1.0 mM $\text{Cu}(\text{ClO}_4)_2/50\text{ mM HClO}_4$ aqueous solution at a scan rate of 10 mV s^{-1} . As expected, the Cu UPD on the bare gold electrode gives a broad deposition peak during the cathodic sweep at about 190 mV and a stripping wave on the anodic scan at 300 mV.^{30,39}

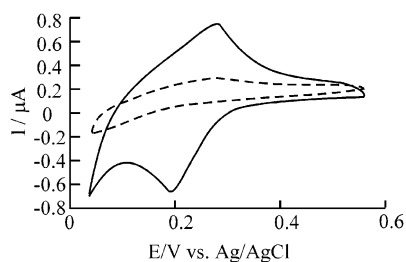


Figure 3. Under potential deposition of copper on bare (—) and ds-DNA-modified gold electrodes (---); 1 mM $\text{Cu}(\text{ClO}_4)_2$ + 0.05 M HClO_4 , scan rate was 10 mV s^{-1} . The gold electrode area was 0.02 cm^2 .

In contrast to bare gold, the UPD of Cu on the ds-DNA-modified gold electrode is strongly suppressed. The amount of charge involved in the stripping wave is decreased by 95% compared to that of the UPD on bare gold ($15 \mu\text{C cm}^{-2}$ as compared to $275 \mu\text{C cm}^{-2}$ for bare gold). These results suggest that the monolayer of ds-DNA prepared from **1** and **2** is well packed and has a limited amount of exposed surface area that is directly accessible to the electrolyte solution.

DNA self-assembled monolayers immobilized on gold electrode surfaces provide an excellent means for studying electron-transfer kinetics through DNA. The electron transfer through the DNA monolayer from solution-based redox couples to the electrode surface is good a measure of the conductivity of the molecular assembly. Anionic $[\text{Fe}(\text{CN})_6]^{3-/4-}$ and cationic $[\text{Ru}(\text{NH}_3)_6]^{3+/4+}$ were chosen to study the electron transfer between a gold surface and a solution-based redox probe. They have been used extensively to study electrode kinetics and to examine solid electrode surfaces.^{36,40} Both exhibit reversible or quasi-reversible but well-behaved redox chemistry in aqueous solution.

Figure 4 shows a series of four cyclic voltammograms of 2.5 mM $[\text{Fe}(\text{CN})_6]^{3-/4-}$ solutions at pH 8.6 using a bare gold working electrode (4a), a ds-DNA-modified gold electrode (4b), a ds-DNA-modified electrode in the presence of 0.3 mM Mg^{2+} (4c), and a ds-DNA-modified electrode in the presence of 0.3 mM Zn^{2+} (4d). As shown in Figure 4a, the CV curve for bare gold shows the reduction and oxidation peaks that are typical for a diffusion-limited one-electron redox process. The CV of ds-DNA on gold shown in Figure 4b exhibits a much reduced signal because of the $[\text{Fe}(\text{CN})_6]^{3-/4-}$ redox couple (only 5% compared to bare gold) in what can be described as an irreversible system with a large peak-to-peak separation (ΔE_p). Thus, the electronic communication between the solution electrophore and the gold surface is effectively suppressed, indicating blocking of the gold surface by the ds-DNA. Electron transfer between the solution electrophore and the gold surface now has to proceed through the ds-DNA/hydroxyl- C_6 monolayer. This increase in distance between the gold surface and the solution electrophore will result in a slower electron-transfer rate, which in CV will result in an increase in ΔE_p . In addition, the electrostatic repulsion between the ds-DNA molecules on the surface and the anionic $[\text{Fe}(\text{CN})_6]^{3-/4-}$ has to be considered, which does not allow for an effective penetration of the monolayer by the negatively charged electrophore. Better blocking was observed by Kelly and co-workers for a monolayer of 5'HS-(CH_2)₆-p-15 base oligonucleotides, which appears to be free of any measurable pinholes and provides complete blocking.⁴¹ Similarly, a monolayer using 418-bp DNA completely blocks the $[\text{Fe}(\text{CN})_6]^{3-/4-}$ electrophore, and no signal transduction was observed.¹⁹ In contrast, our monolayer consists of a 20-bp ds-DNA-hydroxylalkyl disulfide.

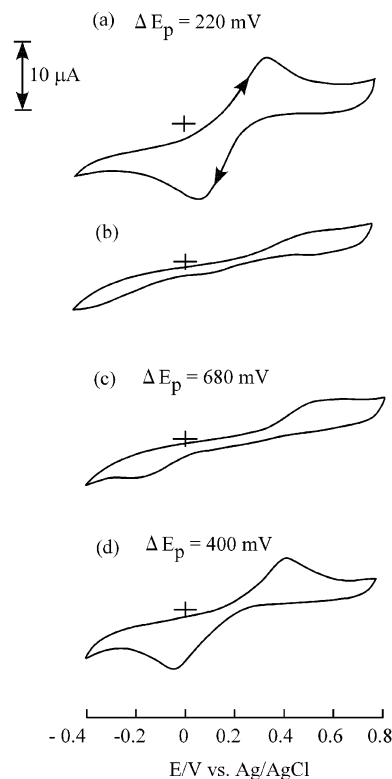


Figure 4. Cyclic voltammograms of bare and ds-DNA-modified electrodes. (a) Bare gold electrode; (b) ds-DNA-coated gold electrode; (c) ds-DNA-modified gold electrode soaked in 0.3 mM MgClO_4 for 2.5 h; (d) ds-DNA-modified gold electrode soaked in a solution containing 0.3 mM $\text{Zn}(\text{ClO}_4)_2$ for 2.5 h. The concentration of ferri-cyanide/ferrocyanide was 2.5 mM in 20 mM tris- ClO_4 buffer (pH 8.6). All CVs were recorded at a sweep rate of 100 mV s^{-1} .

Both residues are deposited on the surface, and the resulting monolayer does not completely block the redox activity of the $[\text{Fe}(\text{CN})_6]^{3-/4-}$ electrophore. We propose that the electron passes through the hydroxyl "defect" sites rather than through the ds-DNA, which may allow for closer proximity between the redox probe and the surface. Because of the charge repulsion between the phosphates and $[\text{Fe}(\text{CN})_6]^{3-/4-}$, monolayer penetration by the solution anion will have a low probability. As demonstrated by the UPD experiments with Cu^{2+} , some of the gold is accessible to the electrolyte, and thus we cannot rule out some contributions from these sites. However, the contribution should be the same for M-DNA and native ds-DNA.

A comparison of a monolayer prepared by the method outlined above to that of a method described by Steel³³ shows a notable difference in the blocking ability. Steel's method, briefly outlined, uses a mixed monolayer system (ss-DNA-SH and C_6 -SH) employing only thiols, and the DNA-hybridization step occurs after the monolayer formation is established. The electrode surface blocking results clearly show that Steel's method produces a surface that can permit electron transfer to the redox probe, whereas a monolayer produced using the method described here is effectively blocked to electron transfer. According to the Steel study, the surface density of ds-DNA was about $(1-10) \times 10^{-12} \text{ mol cm}^{-2}$ of a 25-bp DNA, indicating low surface coverage.³³ On the basis of the small Faradaic current produced from the electrophore, the ds-DNA-SS monolayer appears to be tightly packed, resulting in better insulation of the Au surface electrode.

In contrast, the positively charged $[\text{Ru}(\text{NH}_3)_6]^{3+/4+}$ is not effectively blocked by the ds-DNA. Figure 5 shows a CV curve of a ds-DNA-modified gold electrode and a bare gold electrode

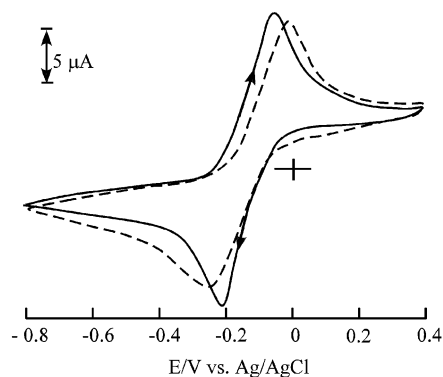


Figure 5. Cyclic voltammograms at bare (—) and ds-DNA-modified electrodes (---) in 5.0 mM hexaammineruthenium(III/IV) chloride in 20 mM tris-ClO₄ buffer (pH 8.6) at a sweep rate of 100 mV s⁻¹.

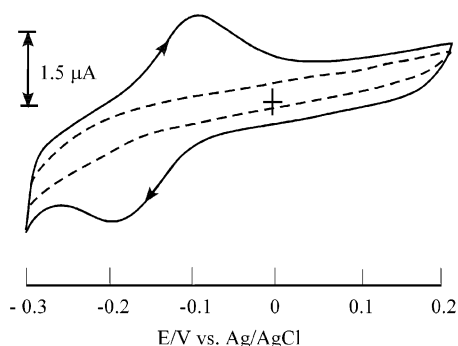


Figure 6. Cyclic voltammograms of ds-DNA-modified gold electrodes in blank buffer (20 mM tris-ClO₄, pH 8.6) after incubation in buffered solutions of ferricyanide/ferrocyanide (---) or hexaammineruthenium(III/IV) chloride (—) and thorough rinsing with buffer at a sweep rate of 100 mV s⁻¹. A Faradaic current was observed only for Ru(NH₃)₆^{3+/4+}.

with the [Ru(NH₃)₆]^{3+/4+} electrophore in solution. Signal transduction through the monolayer proceeds virtually unimpeded. The peak separation ΔE_p is slightly increased from 0.17 to 0.20 V as compared to that of the bare gold electrode. These results suggest that the [Ru(NH₃)₆]^{3+/4+} ion can interact to a significant degree with the electrode surface. Presumably, there is a favorable interaction between the negatively charged phosphate backbone and the positively charged [Ru(NH₃)₆]^{3+/4+} ion, allowing for effective penetration of the monolayer.

In the case of the anionic [Fe(CN)₆]^{3-/4-}, the monolayer is more resistant to ion and electrolyte penetration. Even after washing the [Ru(NH₃)₆]^{3+/4+}-exposed ds-DNA/hydroxyalkyl monolayer with copious amounts of buffer solution, a significant signal due to electroactive [Ru(NH₃)₆]^{3+/4+} is still present in the monolayer. Figure 6 compares the CV curve of [Ru(NH₃)₆]^{3+/4+}-exposed and [Fe(CN)₆]^{3-/4-}-exposed monolayers after extensive rinsing. Note that the [Ru(NH₃)₆]^{3+/4+} signal can still be observed after washing with buffer whereas the signal due to [Fe(CN)₆]^{3-/4-} is completely absent after washing. This is evidence of redox probe penetration or electrostatic charge coupling along the PO₄³⁻ backbone.

The ds-DNA/hydroxyalkyl monolayer shown in Figure 4 effectively blocks the signal transduction of [Fe(CN)₆]^{3-/4-}. The addition of 0.3 mM Mg²⁺ to the buffer at pH 8.6 changes the signal transduction only slightly (Figure 4c). It is expected that Mg²⁺ will coordinate to the phosphate backbone and thereby reduce the electrostatic repulsion, allowing for better ion penetration of the monolayer by [Fe(CN)₆]^{3-/4-}. However, Figure 4d shows that the signal represents only about 10% of

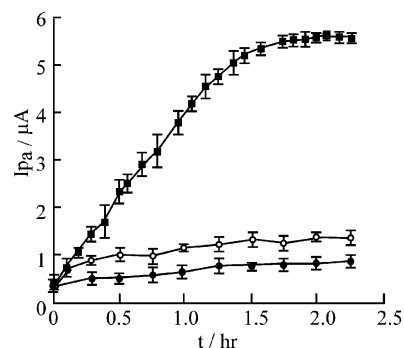


Figure 7. Anodic peak current as a function of incubation time for the ds-DNA-modified electrode in (●) 2.5 mM ferricyanide/ferrocyanide in tris-ClO₄ buffer solution (20 mM, pH 8.6) with the addition of (■) 0.3 mM Zn(ClO₄)₂ or (○) 0.3 mM MgCl₂. The error bars represent the standard deviation on three independent determinations.

the signal intensity on bare gold, with a very large ΔE_p of 0.68 V indicating slow electron transfer between the solution and the surface.

However, upon adding 0.3 mM Zn(ClO₄)₂ to the buffer solution at pH 8.6 to form M-DNA, a large signal due to the [Fe(CN)₆]^{3-/4-} electrophore, which has 80% of the integrated signal intensity compared to that of bare gold (Figure 4d), is observed. The CV curve exhibits a significantly increased signal as compared to that of the blocked ds-DNA monolayer electrode. The peak separation in the presence of Zn²⁺ is larger (ΔE_p = 0.40 V) than that for bare gold (ΔE_p = 0.22 V). Thus, in the presence of Zn²⁺, under favorable M-DNA formation conditions, effective signal transduction takes place from the solution electrophore to the gold electrode. In comparison, the addition of Mg²⁺ does not allow for an effective signal transduction (Figure 4c) under M-DNA conditions. As a final control, adding Zn²⁺ at pH 7.0 does not give rise to increased electron transfer because M-DNA is proposed not to form at this pH.

Figure 7 shows a time study on the effects of the addition of Zn²⁺ and Mg²⁺ on the CV of the ds-DNA/hydroxyalkyl monolayer. Initially, the monolayer is blocking the electron-transfer process effectively. After the addition of Zn²⁺ to the buffer solution, the signal intensity of the CV of the [Fe(CN)₆]^{3-/4-} electrophore in solution steadily increases up to a limit, and the peak separation decreases. Figure 7 shows the time dependence of the anodic peak current with increasing incubation time in the presence of Zn²⁺ or Mg²⁺. For Zn²⁺, the current increases significantly, reaches a maximum after about 2 h, and then remains at this maximum, corresponding to about 80% of the signal intensity of bare gold. For Mg²⁺, the increase over the same period is comparatively small. Thus, the electrochemical properties of the ds-DNA/hydroxyalkyl monolayer in the presence of Mg²⁺ are not affected. The time-dependent increase of the electrical response probably represents the dynamics of the incorporation of Zn²⁺ into the ds-DNA monolayer. To a first approximation, the M-DNA formation on the surface follows pseudo-first-order kinetics with a pseudo-first-order rate constant of $k = 10 \text{ min}^{-1}$.

The anodic peak current exhibits a linear dependence that increases with the square root of the scan rate in the range of 50 to 500 mV (Figure 8), suggesting that the electrochemical reaction is primarily controlled by linear diffusion and not by pinholes or defects.⁴⁰

Thus, the Faradic current is due to electron transfer from the [Fe(CN)₆]^{3-/4-} electrophore through the M-DNA helix to the electrode surface. Figure 9 shows the CV curve of M-DNA in the absence and presence of EDTA. It was shown in previous

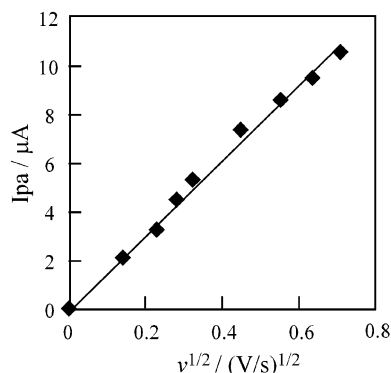


Figure 8. Plot of anodic peak current (I_{pa}) vs the square root of the sweep rate. The cyclic voltammograms were obtained using a gold electrode modified by a M-DNA SAM in 20 mM tris-HClO₄ buffer (pH 8.6) in the presence of 5 mM ferricyanide/ferrocyanide.

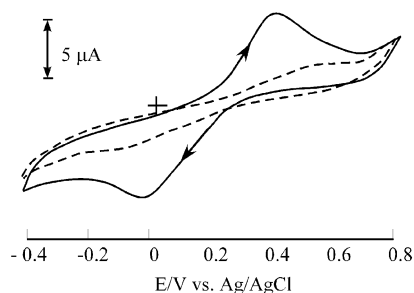


Figure 9. Cyclic voltammograms at M-DNA-modified gold electrodes (—) or after treatment with 1 mM EDTA (---) for 90 min measured in 2.5 mM ferricyanide/ferrocyanide in 20 mM tris-HClO₄ buffer (pH 8.6) at a sweep rate of 100 mV s⁻¹.

studies that EDTA will complex Zn²⁺ and convert back to native ds-DNA.¹⁰ Upon adding EDTA to the buffer containing the M-DNA monolayer, the signal intensity is significantly decreased.

In addition, the peak separation increases, indicating a loss of signal transduction from the [Fe(CN)₆]^{3-/4-} electrophore through the monolayer after the removal of the Zn²⁺ ions. The resulting CV curve exhibits the same features as that of the ds-DNA monolayer. The signal intensity is reduced compared to that of the M-DNA monolayer showing a large ΔE_p (0.60 V). Thus, the M-DNA can be converted back to native ds-DNA on the gold surface.

We evaluated the heterogeneous electron-transfer kinetics for bare gold and the M-DNA modified electrode by comparing the experimental curve with a simulated CV curve. Figure 10 shows the CV curves for a bare Au electrode (Figure 10a) and the M-DNA SAMs' modified Au electrode after ds-DNA SAM background subtraction (Figure 10b) together with the simulated CV plot. The diffusion coefficients for the [Fe(CN)₆]^{3-/4-} redox couple are $D_{ox} = D_{red} = 8 \times 10^{-6}$ cm² s⁻¹.⁴²

In 20 mM tris-HClO₄ buffer at a scan rate of 100 mV s⁻¹, a ΔE_p of 220 mV was measured for the [Fe(CN)₆]^{3-/4-} redox couple at the bare electrode, and a ΔE_p of 400 mV, for the M-DNA monolayer-modified Au electrode. Under these conditions, the electron-transfer rate constant k_{ET} was $9.1 \times 10^{-4} \pm 0.2 \times 10^{-4}$ cm s⁻¹ for the bare Au electrode and $1.2 \times 10^{-4} \pm 0.2 \times 10^{-4}$ cm s⁻¹ for the M-DNA/hydroxylalkyl-modified Au electrode. In the case of the ds-DNA/hydroxylalkyl-modified Au electrode, the electron-transfer rate constant was too small to be measured, thus k_{ET} must be orders of magnitude smaller.

To compare and verify the results obtained from the analysis of the sampled voltammetry, a charge-integration technique, chronocoulometry, was employed on the same set of redox

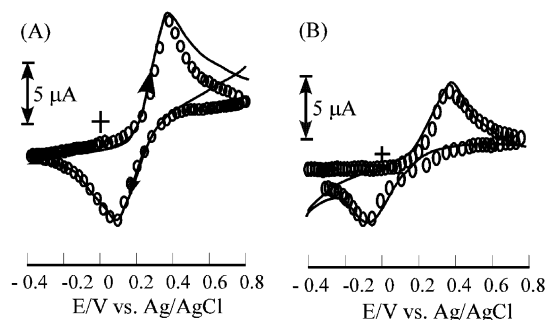


Figure 10. Cyclic voltammograms (—) of 2.5 mM ferricyanide/ferrocyanide in 20 mM tris-HClO₄ buffer solution (pH 8.6) at (A) a bare gold electrode and (B) a M-DNA-modified gold electrode at 25 °C together with simulated data (○). Scan rate used was 100 mV s⁻¹. Digital simulations were made using the k_{ET} , E_0 , and α (transfer coefficient) values of (A) 9.1×10^{-4} , 0.21 vs Ag/AgCl/3 M NaCl, and 0.5 and (B) 1.23×10^{-4} cm s⁻¹, 0.19 V vs Ag/AgCl/3 M NaCl, and 0.4. The diffusion coefficients of D_{ox} and D_{red} used for A were 8×10^{-6} cm² s⁻¹ for ferricyanide and ferrocyanide. Both CVs have the background current subtracted.

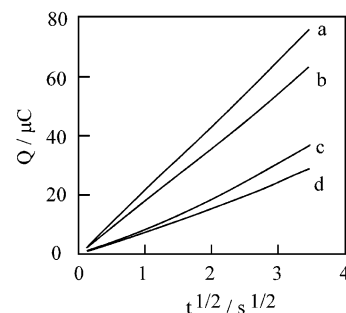


Figure 11. Chronocoulometric transients at -350 mV of 5 mM ferricyanide in 20 mM tris-HClO₄ buffer (pH 8.6) at (a) bare gold, (b) a ds-DNA-modified gold electrode in the presence of 0.3 mM Zn(ClO₄)₂ in the solution, (c) a ds-DNA-modified gold electrode in the presence of 0.3 mM MgClO₄ in the solution, and (d) a ds-DNA-modified electrode.

systems under identical experiment conditions. Recently, several authors have used chronocoulometry to characterize mismatched DNA⁴³ or to determine the surface density of immobilized DNA^{33,44} quantitatively on the basis of the charge transport to the surface. A comparison of the charge passed at the various modified electrodes is shown in Figure 11. The initial potential started at 200 mV versus Ag/AgCl, where no electrolysis of ferricyanide occurs. During a single step of 12 s to the potential of -350 mV at which essentially all of the ferricyanide is reduced to ferrocyanide, the amount of charge passed on the M-DNA-modified electrode is significantly larger than that on the ds-DNA-modified electrode. These experiments confirm the results of CV in that blocking electron transfer of from [Fe(CN)₆]^{3-/4-} through M-DNA is much more effective than through conventional ds-DNA.

In conclusion, we have confirmed by CV and chronocoulometry that blocking electron transfer on a ds-DNA-modified electrode can be overcome by converting to M-DNA, through which electron transfer is much faster. Therefore, M-DNA may find widespread applications in nanoelectronics or biosensing since a direct electrical readout of hybridization or DNA binding is now possible.

Acknowledgment. We thank CIHR, NSERC, and UMDI for financial support. H-B.K. holds the Canada Research Chair in Biomaterials, and J.S.L. is supported by a Senior Investigators

Award from the Regional Partnership Program of CIHR. In addition, we thank Dr. T. Sutherland for helpful discussions.

References and Notes

- (1) Elghanian, R.; Storhoff, J. J.; Mucic, R. C.; Letsinger, R. L.; Mirkin, C. A. *Science (Washington, D.C.)* **1997**, *277*, 1078–1081.
- (2) Bobinson, B. H.; Seeman, N. C. *Protein Eng.* **1987**, *1*, 295–300.
- (3) Gooding, J. J.; Hibbert, D. B.; Yang, W. *Sensors* **2001**, *1*, 75–90.
- (4) Niemeyer, C. M. *Appl. Phys.* **1999**, *68*, 119–124.
- (5) Wilson, E. K. *Chem. Eng. News* **1997**, *24*, 33–39.
- (6) Murphy, C. J.; Arkin, M. R.; Jenkins, Y.; Ghatlia, N. D.; Bossmann, S. H.; Turro, N. J.; Barton, J. K. *Science (Washington, D.C.)* **1993**, *262*, 1025–1029.
- (7) Porath, D.; Bezryadin, A.; de Vries, S.; Dekker, C. *Nature (London)* **2000**, *635*–638.
- (8) Braun, E.; Eichen, Y.; Sivan, U.; Ben-Yoseph, G. *Nature (London)* **1998**, *391*, 775–778.
- (9) Aich, P.; Labiuk, S. L.; Tari, L. W.; Delbaera, L. J. T.; Roesler, W. J.; Falk, K. J.; Steer, R. P.; Lee, J. S. *J. Mol. Biol.* **1999**, *294*, 477–485.
- (10) Lee, J. S.; Latimer, L. J. P.; Reid, R. S. *Biochem. Cell Biol.* **1993**, *162*–168.
- (11) Mikkelsen, S. R. In *Encyclopedia of Electrochemistry*; Bard, A. J., Stratmann, M., Eds.; Wiley-VCH: Weinheim, Germany, 2002; Chapter 11.
- (12) Galka, M. M.; Kraatz, H. B. *ChemPhysChem* **2002**, *3*, 356–359.
- (13) Huang, E.; Zhou, F.; Deng, L. *Langmuir* **2000**, *16*, 3272–3280.
- (14) Thorp, H. H. *Trends Biotechnol.* **1998**, *16*, 117–121.
- (15) Watterson, J. H.; Piumno, P. A. E.; Wust, C. C.; Krull, U. J. *Anal. Chim. Acta* **1999**, *395*, 273–284.
- (16) Palecek, E. *Bioelectrochem. Bioenerg.* **1986**, *15*, 275–295.
- (17) Kelley, S. O.; Barton, J. K.; Jackson, N. M.; Mcpherson, L. D.; Potter, A. B.; Spain, E. M.; Allen, M. J.; Hill, M. G. *Langmuir* **1998**, *14*, 6781–6784.
- (18) Herne, T. M.; Tarlov, M. J. *J. Am. Chem. Soc.* **1997**, *119*, 8916–8920.
- (19) Yang, M.; Yau, H. C. M.; Chan, H. L. *Langmuir* **1998**, *14*, 6121–6129.
- (20) Okahata, Y.; Matsunobu, Y.; Kuniyama, I.; Masayuki, M.; Murakami, A.; Makino, K. *J. Am. Chem. Soc.* **1992**, *114*, 8299–8300.
- (21) Tarlov, M. J.; Newman, J. G. *Langmuir* **1992**, *8*, 1398–1405.
- (22) Nuzzo, R. G.; Allara, D. L. *J. Am. Chem. Soc.* **1983**, *105*, 4481–4483.
- (23) Bain, C. D.; Biebuyck, H. A.; Whitesides, G. M. *Langmuir* **1989**, *5*, 723–727.
- (24) (a) Schonherr, H.; Ringsdorf, H.; Jaschke, M.; But, H.-J.; Bamberg, E.; Allinson, H.; Evans, S. D. *Langmuir* **1996**, *12*, 3898. (b) Biebuyck, H. A.; Whitesides, G. M. *Langmuir* **1993**, *9*, 1766–1770. (c) Ishida, T.; Yamamoto, S.; Mizutani, W.; Motomatsu, M.; Tokumoto, H.; Hokari, H.; Azebara, H.; Fujihara, M. *Langmuir* **1997**, *13*, 3261–3265.
- (25) Wincoff, F.; Drenzo, A.; Shaffer, C.; Sweedler, D.; Gonzalez, C.; Scarinje, S.; Usman, N. *Nucleic Acids Res.* **1995**, *25*, 2677–2684.
- (26) Hallmark, V. M.; Chiang, S.; Rabolt, J. F.; Swalen, J. D. *Phys. Rev. Lett.* **1987**, *59*, 2879.
- (27) Woods, R.; Bard, A. J.; Dekker, M. 1 ed.; New York, 1980; Chapter 9.
- (28) Pecq, J. B. L.; Paoletti, C. *Anal. Biochem.* **1966**, *17*, 100–107.
- (29) Eliadis, E. D.; Nuzzo, R. G.; Gewirth, A. A.; Alkire, R. C. *J. Electrochem. Soc.* **1997**, *144*, 96–105.
- (30) Sun, L.; Crooks, R. M. *J. Electrochem. Soc.* **1991**, *138*, L23–L25.
- (31) Nishizawa, M.; Sunagawa, T.; Yoneyama, H. *Langmuir* **1997**, *13*, 5215–5217.
- (32) Satjapipat, M.; Sanedrin, R.; Zhou, F. *Langmuir* **2001**, *17*, 7637–7644.
- (33) Steel, A. B.; Herne, T. M.; Tarlov, M. J. *Anal. Chem.* **1998**, *70*, 4670–4677.
- (34) Steel, A. B.; Levicky, R. L.; Herne, T. M.; Tarlov, M. J. *Biophys. J.* **2000**, *79*, 975–981.
- (35) Zamborini, F. P.; Crooks, R. M. *Langmuir* **1998**, *14*, 3279–3286.
- (36) Takehara, K.; Takemura, H.; Ide, Y. *Electrochim. Acta* **1994**, *39*, 817–822.
- (37) Cha, X.; Ariga, K.; Kunitake, T. *Bull. Chem. Soc. Jpn.* **1996**, *69*, 163–168.
- (38) Clegg, R. S.; Hutchinson, J. E. *Langmuir* **1996**, *12*, 5239–5243.
- (39) Sondag-Huethorst, J. A. M.; Fokkink, L. G. J. *Langmuir* **1995**, *11*, 4823–4831.
- (40) Chailapakul, O.; Crooks, R. M. *Langmuir* **1993**, *9*, 884–888.
- (41) Kelley, S. O.; Barton, J. K.; Jackson, N. M.; Hill, M. G. *Bioconjugate Chem.* **1997**, *8*, 31–37.
- (42) Winkler, K. *J. Electroanal. Chem.* **1995**, *388*, 151–159.
- (43) Kelley, S. O.; Boon, E. M.; Barton, J. K.; Jackson, N. M.; Hill, M. G. *Nucleic Acids Res.* **1999**, *27*, 4830–4837.
- (44) Patolsky, F.; Lichtenstein, A.; Willner, I. *J. Am. Chem. Soc.* **2001**, *123*, 5194–5205.